

This is the accepted manuscript made available via CHORUS. The article has been published as:

Evolution of the spin-state transition with doping in  
 $\text{La}_{1-x}\text{Sr}_x\text{CoO}_3$

R. X. Smith, M. J. R. Hoch, W. G. Moulton, P. L. Kuhns, A. P. Reyes, G. S. Boebinger, H. Zheng, and J. F. Mitchell

Phys. Rev. B **86**, 054428 — Published 20 August 2012

DOI: [10.1103/PhysRevB.86.054428](https://doi.org/10.1103/PhysRevB.86.054428)

# Evolution of the spin state transition with doping in $\text{La}_{1-x}\text{Sr}_x\text{CoO}_3$

R.X. Smith, M.J.R. Hoch, W.G. Moulton, P.L. Kuhns, A.P. Reyes, G.S. Boebinger  
*National High Magnetic Field Laboratory, Florida State University, Tallahassee, Florida 32310, USA*

H. Zheng, J.F. Mitchell  
*Materials Science Division, Argonne National Laboratory, Argonne, Illinois 60439, USA*  
(Dated: July 13, 2012)

The thermally induced spin state transition of  $\text{Co}^{3+}$  ions in the cobaltite  $\text{LaCoO}_3$ , found at temperatures in the range 40 to 120 K, has been the subject of extensive experimental and theoretical investigation. Much less is known about what happens to the spin state transition in hole-doped  $\text{La}_{1-x}\text{Sr}_x\text{CoO}_3$  (LSCO). The present  $^{139}\text{La}$  NMR experiments show that spin-state transitions persist in nanoscale hole-poor regions of the inhomogeneous doped material. In fact, thermally-induced spin-state transitions remain important for doping levels close to the metal-insulator critical concentration of  $x_C = 0.17$ . This finding suggests that the unusual glassy behavior seen in doped LSCO for  $x < 0.18$  results from the interplay of spin-state transitions in hole-poor regions and ferromagnetism in hole-rich regions.

PACS numbers: 76.60.-k 75.50.Lk 75.47.Lx

The hole-doped cobaltite,  $\text{La}_{1-x}\text{Sr}_x\text{CoO}_3$ <sup>1</sup>, evolves with increase in  $x$  from a parent insulating compound,  $\text{LaCoO}_3$ , in which the  $\text{Co}^{3+}$  ions undergo a thermally induced spin-state transition across a  $\sim 12$  meV energy gap, to become a spin-glass at low doping and a ferromagnet at high doping. At the critical doping of  $x_C = 0.17$ , the system simultaneously undergoes a percolative insulator-to-metal transition (IMT) and ferromagnetic (FM) order transition. The IMT results from the overlapping of metallic spin-clusters that emerge from the close proximity of multiple randomly doped Sr ions<sup>2,3</sup>.

NMR provides a powerful means for detecting local magnetic inhomogeneities from the measured local hyperfine (internal magnetic) field distribution:  $^{139}\text{La}$  NMR spectra from single crystal samples show a doping-dependent distribution of hyperfine couplings consistent with nanoscale phase separation between hole-poor and hole-rich regions<sup>2,4</sup>. We report NMR measurements of spin relaxation rates that reveal the important role of spin-state transitions in hole-poor regions that: (1) persist to much higher doping than previously reported from bulk measurements<sup>5</sup>, and can therefore (2) interact with adjacent magnetic clusters.

In the undoped parent compound,  $\text{LaCoO}_3$ , spin-state transitions result from the crystal field splitting of the Co d-shell that creates a  $\sim 12$  meV gap between the  $e_g$  and  $t_{2g}$  orbitals.  $\text{Co}^{3+}$  contains six electrons in its outer d-shell that fill the  $t_{2g}$  orbitals yielding an  $S=0$  ground state, referred to as the low-spin (LS) state. The small crystal field splitting allows the  $t_{2g}$  electrons to be thermally excited into the  $e_g$  orbitals and thus a higher spin state. Current studies seek to determine whether this excited spin-state is  $S=1$  or  $S=2$ <sup>6-9</sup>, referred to as the intermediate spin (IS) or high spin (HS) state, respectively. Evidence for spin-state transitions comes almost entirely from measurements on the parent compound  $\text{LaCoO}_3$ .

Substituting divalent  $\text{Sr}^{2+}$  ions for trivalent  $\text{La}^{3+}$  ions results in spin polarons<sup>2,10</sup>. Neighboring Co ions with

mixed valency ( $\text{Co}^{3+}$  and  $\text{Co}^{4+}$ ) interact ferromagnetically via the double exchange (DE) interaction<sup>11,12</sup>. As doping increases the spin-polarons merge and form short-range FM clusters<sup>2,13,14</sup>.

We present high-field  $^{139}\text{La}$  NMR spin relaxation measurements that probe the temperature-dependent spin dynamics of LSCO for a range of doping,  $0 < x < 0.30$ , that spans the spin glass, IMT, and FM concentration range. We measure a set of floating zone grown single crystal  $\text{La}_{1-x}\text{Sr}_x\text{CoO}_3$  samples with  $x=0.05, 0.10, 0.15, 0.18, 0.25$  and  $0.30$ . Measurements on a polycrystalline powder of  $x=0$  were also made. All samples were crushed to a grain size of  $\sim 20$  microns to maximize RF penetration into the sample. The  $^{139}\text{La}$  ( $I=7/2$ ;  $^{139}\gamma/2\pi = 6.015$  MHz/T) relaxation rate measurements were made with a pulsed NMR spin echo spectrometer operating at 84.2 MHz in an applied magnetic field of 11 - 14 T. The hyperfine field (0 to 3 T) at  $^{139}\text{La}$  sites in the doped samples acts anti-parallel to the applied field. Due to negligible spectral weights at higher temperatures  $W_2$  and  $W_1$  were measured at only one of two selected points in the spectra corresponding to hyperfine fields of either 0 T or 2 T for all dopings except for  $x=0.15$  where it was possible to measure for both fields.

The near-cubic lattice structure yields a transferred hyperfine field, from the eight nearest neighbor (nn) electron spins on the nn Co ions, at a La nuclear site<sup>4</sup>. The Hamiltonian is  $\mathcal{H}_{hf} = \sum_i \mathbf{S}_i \hat{A}_i \mathbf{I}$  with  $I=7/2$  the nuclear spin,  $\mathbf{S}_i$  the eight nearest neighbor electron spins at Co ion sites  $i$  and  $\hat{A}_i$  the corresponding transferred hyperfine coupling tensor produced by orbital hybridization. In this work we neglect the small quadrupolar coupling. The  $T$  dependence of the spin-lattice  $W_1$  and spin-spin  $W_2$  relaxation rates for undoped  $\text{LaCoO}_3$  are shown in Fig.1(a) while Fig.1(b) shows these rates for the metallic sample  $\text{La}_{0.7}\text{Sr}_{0.3}\text{CoO}_3$ . The  $W_2$  dephasing curves are well fit with a single exponential function for all dopings while the  $W_1$  relaxation curves exhibit stretched ex-

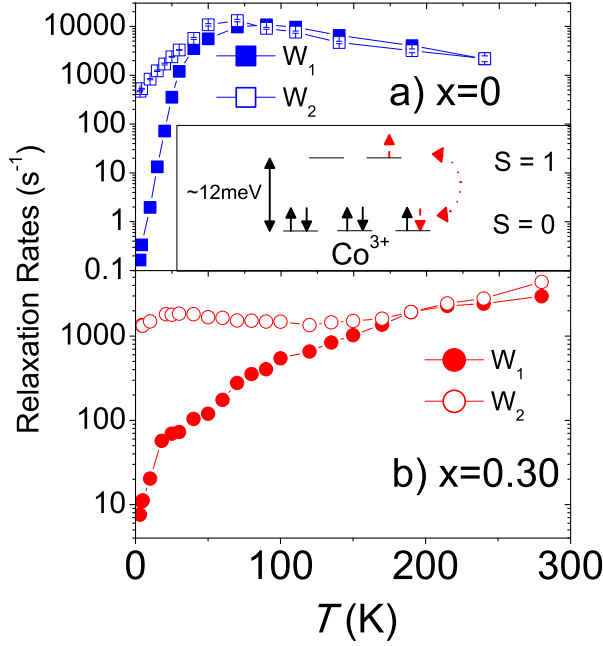


FIG. 1. a) Temperature dependence of  $W_1$  and  $W_2$  measured at a fixed hyperfine field of 0 T for the undoped parent compound,  $\text{LaCoO}_3$ . The inset shows the spin-state transition that dominates  $W_1$  and  $W_2$  in the undoped system. b)  $W_1$  and  $W_2$  measured at a fixed hyperfine field of 2 T for the heavily doped,  $x=0.30$ , ferromagnetic system.

ponential behavior except at the highest temperatures where they are single exponential. Figures 2(a-e) give the behavior of  $W_2$  with  $T$  for  $x$  in the range 0.05 to 0.25 at magnetic fields that correspond to the selected hyperfine shifts  $B_{hf}$  that are shown in the 4.2 K spectra displayed as inserts. The contour plots in the right column of Fig. 2 show the  $^{139}\text{La}$  hyperfine field distributions of a 2D slice of a lattice calculated from the simple statistical model reported in<sup>2</sup>. The contour color mapping correlates to the color mapping under spectra. The blue areas signify hole-poor regions with very low hyperfine fields (i.e. spectral weight at 0 T arises from nuclei situated in regions of zero electronic spin polarization) and the red/white regions indicate hole-rich FM regions with high hyperfine fields ( $>2$  T). The green/yellow regions map the intermediate hyperfine field ( $0 < \text{HF} < 2$  T) regions that separate the hole-poor and hole-rich regions.

The temperature dependence of  $W_1$  in the parent compound,  $x=0$ , (Fig.1a) shows a large increase,  $\sim 6$  orders of magnitude, from 4.2 K to 100 K that has been previously explained in terms of spin-state transitions<sup>15</sup>.  $W_2$  for  $x=0$  displays a similar temperature dependence above 60 K as  $W_1$ , but only experiences an order of magnitude decrease at low temperature. Both the  $W_1$  and  $W_2$  relaxation mechanisms involve fluctuating hyperfine fields with short correlation times due to thermally induced transitions from  $S = 0$  to higher spin excited states and to spin transitions within the manifold of Zeeman split

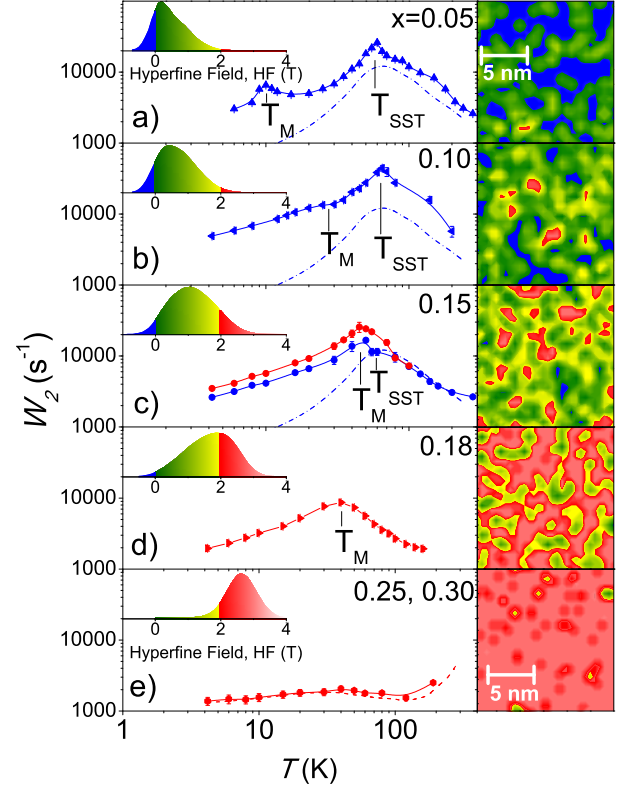


FIG. 2. Temperature dependence of the spin-spin relaxation rate,  $W_2$ , for a range of dopings,  $x$ , for both hole-poor regions (measured at  $\text{HF}=0$  and shown in blue) and hole-rich regions (measured at  $\text{HF}=2$  T and shown in red). Data for  $x=0$  are plotted as a dash-dot line in a)-c) for comparison. e) contains data for both  $x=0.25$  and  $x=0.30$  (red circles and dashed line, respectively). The peak  $T_{\text{SST}}$  60 K arises from thermally-induced spin-state transitions, which do not change with doping. The  $T_M$  peak arises from the critical fluctuations of a magnetic ordering in the spin-glass regions. The spectra at left in each panel show the  $^{139}\text{La}$  lineshape measured at 4.2 K. The color-coded panels at right are 2-D cross sections of the local moment calculated in a model system from<sup>2</sup>. The color coding from blue (undoped) to red (highly doped) indicates the strength of the internal magnetic field and is common among all measured  $^{139}\text{La}$  lineshapes and model calculations.

excited states. The relaxation rates  $W_1$  and  $W_2$  for the parent compound,  $\text{LaCoO}_3$ , in the short correlation time limit  $\omega_e \tau \ll 1$

$$W_1 \propto \gamma^2 \langle B_{\perp}^2 \rangle \tau, \quad (1)$$

$$W_2 \propto \gamma^2 \left( \langle B_{\perp}^2 \rangle + 2 \langle B_{\parallel}^2 \rangle \right) \tau, \quad (2)$$

where  $\tau$  is the electronic correlation time describing the electronic spin fluctuations,  $\omega_e$  the electron Larmor frequency, and  $B_{\perp}$  and  $B_{\parallel}$  are the transverse and parallel components of the hyperfine field, respectively. These field quantities are dependent on  $\langle S \rangle_{\text{loc}}$ , the average of the spins  $S_i$  on the neighboring Co ions, which has

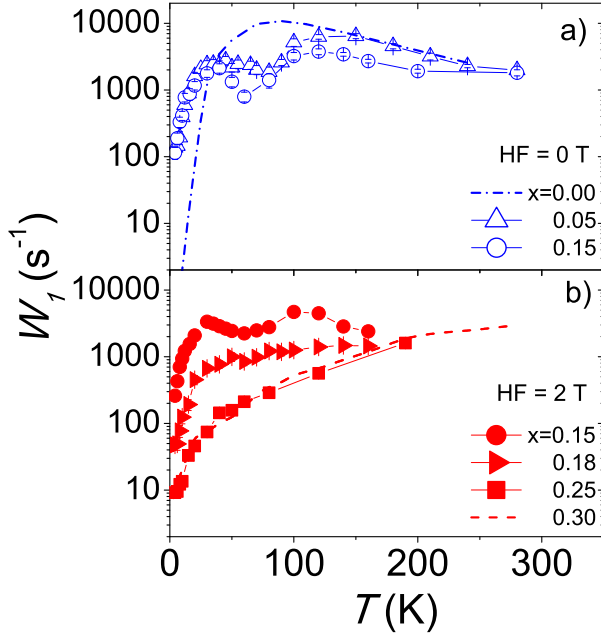


FIG. 3. a) Comparison of the temperature dependence of the spin-lattice relaxation rate,  $W_1$ , for hole-poor regions (blue) and hole-rich (red) measured at a fixed hyperfine field of 0 T for 0.05, and 0.15. The dash-dot line is  $W_1$  for  $x=0$ . b)  $W_1$  measured at a fixed hyperfine field of 2 T for  $x=0.15$ , 0.18, 0.25. The  $W_1$  data for 0.30 is plotted as a dashed line.  $W_1$  deviates from  $x=0$  behavior in  $x=0.05$  and  $x=0.15$ , whereas  $W_2$  shows little deviation. This indicates a change in anisotropy of the relaxation mechanisms.

a temperature dependence governed by the spin-state transition<sup>15</sup>. The temperature at the  $W_2$  peak is determined by the crystal field gap separating the low-spin and higher-spin states. The large difference in the  $W_1$  and  $W_2$  relaxation rates at low temperatures ( $<20$  K) is accounted for as follows. Nuclear dipole-dipole interactions between Co nuclei lead to irreversible dephasing of spins and determine the lower limit of  $W_2$  while no lower limit applies to  $W_1$ .

As expected, the relaxation behavior of the  $x=0.30$  FM metallic sample (Fig.1b) shows markedly different behavior to  $x=0$ . For  $x=0.30$ ,  $W_1 \propto T$ , and  $W_2$  remains roughly temperature independent below the FM ordering temperature  $T_C \sim 225$  K.

Figure 2(a-c) show  $W_2$ 's taken at 0 T hyperfine field (blue regions) for  $x=0$ , 0.05, 0.10, 0.15 (open blue circles). The insets show the  $^{139}\text{La}$  spectra at 4.2 K reported previously<sup>2</sup>. The main results reported here are the broad peaks at 60 K for  $x=0.05$ , 0.10 and 0.15 that reveal the existence of spin-state transitions in hole-poor (blue) regions not previously detected in other measurements. For  $x=0.05$  - 0.10 LSCO the maximum in the  $W_2$  vs.  $T$  plot in Fig. 2 is sharper and somewhat enhanced compared to the values for undoped LCO which

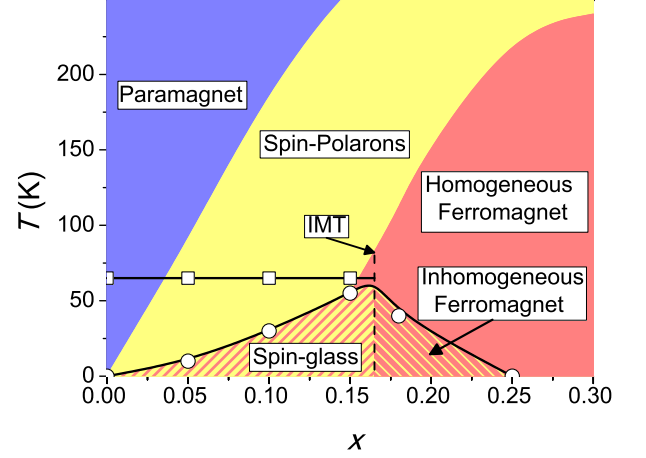


FIG. 4. The  $\text{La}_{1-x}\text{Sr}_x\text{CoO}_3$  phase diagram. The open squares mark the spin-state transition temperature seen in the hole-poor regions. The open circles and red/yellow hashed area indicate the magnetic ordered region that agrees with the spin-glass and spin incommensurate regions seen by susceptibility and neutron scattering measurements. The blue area indicates the region where the system is a paramagnet. The yellow area indicates the region where spin-polarons are nucleating around Sr dopants. The red area represents the region where the system exhibits long-range FM order. The boundaries between the colored regions are determined according to NMR measurements<sup>2</sup>. The dashed vertical line at  $x=0.17$  shows the IMT.

are shown, for comparison, as the dashed curve. The observed differences in the  $T$ -dependent behavior of  $W_2$  with  $x$  can be qualitatively accounted for as follows. In undoped LCO the local environment of the  $\text{Co}^{3+}$  ions is different to that in the inhomogeneous doped samples where nanoscale undoped and hole-doped regions coexist as depicted in the color-coded panel in Fig. 2.  $W_2$  at 0 T for  $x > 0$  involves contributions from undoped small regions in which the spin gap persists, with associated thermally induced spin-state fluctuations, and from dynamical hole-doped small spin clusters, or spin-polarons, with an average static hyperfine field of  $\sim 0$  T. Evidence for spin-polaron dynamics can be inferred from the  $T$  dependence of the  $^{139}\text{La}$  LSCO spectra given in Ref.<sup>2</sup>. The number of polarons increases with  $T$  as large clusters break up and this could lead to a sharpening of the  $W_2$  maximum. The phase separated dynamical behavior occurs for  $0 < x < 0.15$ . At  $x = 0.15$  the  $W_2$  measurements for hyperfine fields of 0 T and 2 T suggest that the spin polaron contribution is now of dominant importance.

The doped samples exhibit an additional peak,  $T_M$ , corresponding to the static ordering of incommensurate short-range spin structures below an ordering temperature,  $T_I < T_C$ , seen by low temperature elastic neutron scattering<sup>16</sup>.  $T_M$  tracks  $T_I$  and vanishes by  $x=0.25$ , in agreement with the incommensurate spin structures gradually disappearing in the same doping range.  $T_M$  and  $T_{SST}$  are almost superimposed at  $x=0.15$ , near the

IMT, suggesting that the value of  $T_M$  is regulated by magnetic interactions between hole-poor and hole-rich regions. We point out that these incommensurate structures coexist with hole-rich clusters, in which FM correlations are present. Figures 2(c-e) show  $W_2$  taken at 2 T hyperfine field (red) for  $x=0.15, 0.18$ , and  $0.25$ .  $W_1$  and  $W_2$  in the strongly FM metallic samples,  $x=0.25$  and  $0.30$ , exhibit a strong upturn above  $\sim 150$  K due to spin fluctuations as  $T_C \sim 250$  K is approached.

Figure 3(a) shows  $W_1$  taken at 0 T hyperfine field for  $x=0-0.15$ . Figure 3(b) shows  $W_1$  taken at 2 T hyperfine field for  $x=0.15-0.30$  (dashed red line). Analogous to the  $W_2$   $T$ -dependent behavior,  $W_1$  at  $B_{hf} = 0$  T involves contributions from both spin-state transitions in undoped nano-regions and from dynamical spin polaron regions. In LSCO for  $T < 10$  K, well below the temperature at which spin state transitions become important, both  $W_1$  and  $W_2$  are much greater than in undoped LCO consistent with nuclear relaxation induced by fluctuating spin polarons in lightly hole-doped regions. It is likely that for the dynamical polarons  $\omega_e\tau > 1$  at the lowest temperatures shown. As mentioned above, the nuclear magnetization recovery exhibits stretched exponential behavior which implies a distribution of relaxation rates in this inhomogeneous material because of the polaron size distribution. As  $T$  is raised the magnetic fluctuations enter the fast correlation time limit  $\omega_e\tau < 1$ , resulting in a decrease in nuclear relaxation rates in the polaron environments as given by Eq. 2. Furthermore, the fraction of nuclei at  $B_{hf} = 0$  T in the dynamic polaron regions, which have reduced  $W_1$  values, increases as  $T$  increases, and this

contribution suppresses the measured average  $W_1$ . The subsequent upturn in  $W_1$  above  $\sim 75$  K, where the rates start to approach the  $x=0$  high- $T$  values, corresponds to large-scale melting of spin clusters and coincides with the transition from stretched to single exponential recovery. We note that the transition to a homogeneous distribution of nuclear relaxation rates also coincides with the increasing importance of hyperfine fluctuations arising from thermally induced hole hopping processes which play a role in transport behavior in the insulating material. The electrical conductivity for  $x=0.05$  and  $x=0.15$  LSCO increases for  $T > 100$  K<sup>17</sup>.

The main finding of this work is the persistence of spin-state transitions in the hole-poor regions of the doped compounds for  $x$  approaching 0.15. The primary experimental evidence for this conclusion is the occurrence of the broad peak  $T_{SSR}$  in the  $W_2$  data at  $\sim 60$  K in Fig. 2 for hole-poor regions ( $HF=0$  T) of doped LSCO that persists up to  $x=0.15$ . This finding is supported by recent theoretical calculations<sup>18</sup>. Hence what has until now been understood to be an insulating spin-glass phase in fact includes the spin-state transitions in hole-poor regions. Figure 4 gives the phase diagram for LSCO based on available information and incorporating the present results. The persistence of spin-state transitions in the insulating phase is shown.

#### ACKNOWLEDGMENTS

Research supported by the U.S. Department of Energy Office of Science, Division of Materials Science and Engineering under Award No. DE-AC02-06CH211357 (crystal growth and characterization).

- 
- <sup>1</sup> J. Wu and C. Leighton, Physical Review B, **67**, 174408 (2003).
  - <sup>2</sup> R. Smith, M. Hoch, P. Kuhns, W. Moulton, A. Reyes, G. Boebinger, J. Mitchell, and C. Leighton, Phys. Rev. B, **78**, 092201 (2008).
  - <sup>3</sup> D. N. H. Nam, R. Mathieu, P. Nordblad, N. V. Khiem, and N. X. Phuc, Phys. Rev. B, **62**, 8989 (2000).
  - <sup>4</sup> M. J. R. Hoch, P. L. Kuhns, W. G. Moulton, A. P. Reyes, J. Lu, J. Wu, and C. Leighton, Phys. Rev. B, **70**, 174443 (2004).
  - <sup>5</sup> S. Yamaguchi, Y. Okimoto, and Y. Tokura, Physical Review B, **55**, R8666 (1997).
  - <sup>6</sup> M. W. Haverkort, Z. Hu, J. C. Cezar, T. Burnus, H. Hartmann, M. Reuther, C. Zobel, T. Lorenz, A. Tanaka, N. B. Brookes, H. H. Hsieh, H.-J. Lin, C. T. Chen, and L. H. Tjeng, Phys. Rev. Lett., **97**, 176405 (2006).
  - <sup>7</sup> M. J. R. Hoch, S. Nellutla, J. van Tol, E. S. Choi, J. Lu, H. Zheng, and J. F. Mitchell, Phys. Rev. B, **79**, 214421 (2009).
  - <sup>8</sup> R. F. Klie, J. C. Zheng, Y. Zhu, M. Varela, J. Wu, and C. Leighton, Phys. Rev. Lett., **99**, 047203 (2007).
  - <sup>9</sup> D. P. Kozlenko, N. O. Golosova, Z. Jiráček, L. S. Dubrovinsky, B. N. Savenko, M. G. Tucker, Y. Le Godec, and V. P. Glazkov, Phys. Rev. B, **75**, 064422 (2007).
  - <sup>10</sup> A. Podlesnyak, M. Russina, A. Furrer, A. Alfonsov, E. Vavilova, V. Kataev, B. Büchner, T. Strässle, E. Pomjakushina, K. Conder, and D. I. Khomskii, Phys. Rev. Lett., **101**, 247603 (2008).
  - <sup>11</sup> C. Zener, Physical Review, **82**, 403 (1951).
  - <sup>12</sup> P. W. Anderson and H. Hasegawa, Physical Review, **100**, 675 (1955).
  - <sup>13</sup> R. Caciuffo, D. Rinaldi, G. Barucca, J. Mira, J. Rivas, M. A. Seánarís Rodríguez, P. G. Radaelli, D. Fiorani, and J. B. Goodenough, Phys. Rev. B, **59**, 1068 (1999).
  - <sup>14</sup> D. Phelan, D. Louca, S. Rosenkranz, S.-H. Lee, Y. Qiu, P. J. Chupas, R. Osborn, H. Zheng, J. F. Mitchell, J. R. D. Copley, J. L. Sarrao, and Y. Moritomo, Phys. Rev. Lett., **96**, 027201 (2006).
  - <sup>15</sup> M. J. R. Hoch, P. L. Kuhns, W. G. Moulton, A. P. Reyes, M. A. Torija, J. F. Mitchell, and C. Leighton, Phys. Rev. B, **75**, 104421 (2007).
  - <sup>16</sup> D. Phelan, D. Louca, K. Kamazawa, S.-H. Lee, S. N. Ancona, S. Rosenkranz, Y. Motome, M. F. Hundley, J. F. Mitchell, and Y. Moritomo, Phys. Rev. Lett., **97**, 235501 (2006).
  - <sup>17</sup> J. Wu, H. Zheng, J. F. Mitchell, and C. Leighton, Physical Review B, **73**, 020404 (2006).
  - <sup>18</sup> A. O. Sboychakov, K. I. Kugel, A. L. Rakhmanov, and

D. I. Khomskii, Phys. Rev. B, **80**, 024423 (2009).